

# The Role of Robust Generalization in Continual Learning: Better Transfer and Less Forgetting

Zenglin Shi<sup>1</sup>, Ying Sun<sup>1,2</sup>, Joo Hwee Lim<sup>1,2,3</sup>, Mengmi Zhang<sup>1,2,3</sup>

<sup>1</sup> I2R, Agency for Science, Technology and Research, Singapore

<sup>2</sup> CFAR, Agency for Science, Technology and Research, Singapore

<sup>3</sup> Nanyang Technological University, Singapore

## Abstract

This paper considers learning a sequence of tasks continually with the objectives of generalizing over unseen data regardless of its distribution, accumulating knowledge and transferring knowledge across tasks. To the best of our knowledge, no existing technique can accomplish all of these objectives simultaneously. This paper proposes such a technique by investigating the role of robust generalization in Continual Learning (CL). Recent findings show that models trained to exhibit robust generalization not only generalize better, but also demonstrate improved transferability and tend to find flatter local minima. This motivates us to achieve robust generalization in each task in CL, facilitating learning a new task and reducing the risk of forgetting previously learned tasks. To achieve this, we propose a new online shape-texture self-distillation (STSD) method that learns both shape and texture representations for each task, improving robust generalization. Extensive experiments demonstrate that our approach can be easily combined with existing CL methods to improve generalization, encourage knowledge transfer, and reduce forgetting. We also show that our approach finds flatter local minima, further highlighting the importance of improving robust generalization in CL. Our proposed technique is a significant step forward in achieving the aforementioned CL objectives simultaneously.

## 1. Introduction

Developing machines that can learn a sequence of tasks continually is a significant challenge in the field of artificial intelligence. An ideal continual learning (CL) model can 1) perform well on the current task, regardless of whether the testing data comes from the same distribution as the training data or not, 2) accumulate knowledge without forgetting previously learned tasks, and 3) transfer knowledge from past tasks to facilitate learning

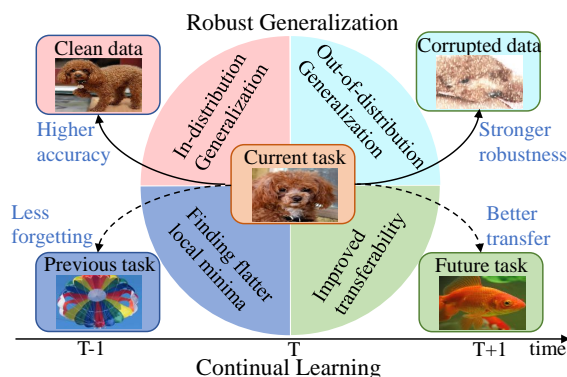


Figure 1: **Integrating robust generalization into continual learning (CL) can yield significant benefits.** CL models with robust generalization ability not only achieve higher task accuracy and stronger robustness to distribution-shift data in each task, but also minimize forgetting about previous tasks and facilitate knowledge transfer to new tasks. The characteristics of robust generalization ability are presented in four sectors of the pie chart. The four round corner rectangles pointed by the four arrows indicate the benefits which a robust generalization model would bring to CL. The two arrows with solid lines and dashed lines denote direct and underlying benefits, respectively.

new tasks. However, current CL techniques do not possess all three capabilities simultaneously. Here, to achieve these objectives, we investigate the role of *robust generalization* in CL, addressing the problems of both in-distribution and out-of-distribution generalization.

Despite that robust generalization and CL are seemingly disjoint topics, for the first time, building upon existing literature, we establish links between the two topics, and provide new insights into why robust generalization can enhance CL abilities (Fig. 1). First, the robust generalization models exhibit the ability to generalize to both in-distribution and out-of-distribution data, which is critical for an ideal CL system. Moreover, these robust generalization models

demonstrate improved transferability [13, 38], which is essential for CL models to quickly adapt to new tasks. Additionally, robust generalization leads to flatter local minima in loss landscapes [41]. Subsequently, flatter local minima reduce the risk of degrading performance on previously learned tasks, as finding flatter local minima in learning each task can effectively mitigate catastrophic forgetting in CL [34, 4, 40, 7].

Many CL methods focus on preventing catastrophic forgetting, where the neural network easily forgets the knowledge of old tasks while learning a new task [33, 14]. To overcome this problem, researchers have explored the following research lines: regularization-based methods [23, 49, 2], knowledge distillation-based methods [27, 3, 46, 11, 35], replay-based methods [37, 36, 3, 46, 18, 30], and flatter local minima-based methods [34, 4, 40, 7]. Recent studies have also proposed methods to encourage knowledge transfer to improve CL performance [22, 28, 29, 5]. This paper proposes a new method to boost robust generalization in each task in CL, leading to better transfer and less forgetting. It can be easily integrated with existing CL methods to further enhance their performance.

Achieving robust generalization is a challenging task, as focusing exclusively on in-distribution or out-of-distribution generalization can result in poor performance in the other, as shown in [50, 9, 6, 13, 16, 17, 45, 47]. Lopes *et al.* [31] make an attempt towards robust generalization by proposing a patch Gaussian augmentation scheme, but its effectiveness is limited to simple image corruptions and yields only marginal accuracy gains. Later, Li *et al.* [26] proposed shape-texture debiased training with a mixup loss to avoid representation learning being overly biased towards shape or texture, balancing in-distribution and out-of-distribution generalizations. While this method displays potential in attaining robust generalization for static learning, it falls short in continual learning (CL) settings where mixup loss impedes CL performance as noted in [35]. To resolve this problem, we introduce a novel online shape-texture self-distillation technique that facilitates learning of both shape and texture representations for CL, leading to better robust generalization. This approach avoids the use of a mixup loss and instead relies on self-distillation.

To summarize, we highlight the following contributions. (I) We investigate the potential of robust generalization to reduce forgetting and promote knowledge transfer in CL, establishing a connection between these two concepts. This is the first time such a relationship has been explored. (II) We propose a new online shape-texture self-distillation technique that enables the simultaneous learning of shape and texture representations in each task, specifically catered for CL scenarios; (III) We conduct extensive experiments to demonstrate the effectiveness of our approach in combination with existing CL methods. Our results

show significant improvements in robust generalization, knowledge transfer, and reduced forgetting. Additionally, our method manages to find flatter local minima, providing further insights into the underlying reason why robust generalization enhances CL.

## 2. Related work

### 2.1. Continual learning

The majority of current CL methods focus on preventing catastrophic forgetting and encouraging knowledge transfer. Notable approaches addressing catastrophic forgetting include the following. 1) Regularization-based approaches, *e.g.*, [23, 49, 2], attempt to overcome this issue by imposing constraints on model parameters. 2) Knowledge distillation-based methods, *e.g.*, [27, 3, 46, 11, 35], typically store a snapshot of the model learned from old tasks and distill the knowledge from the old model to the current model. 3) Replay-based methods, *e.g.*, [36, 3, 46, 18], store a small set of exemplars from old tasks in a memory buffer and then combine it with new data for learning a new task. 4) Flatter local minima-based methods *e.g.*, [34, 4, 40, 7], regulate the flatness of the weight loss landscape of each task.

Several recent studies have shifted their focus toward improving knowledge transfer. For instance, Lin *et al.* [29] proposed a trust region gradient projection method that employs a scaling matrix to facilitate forward knowledge transfer from correlated old tasks to the new task. In a mixed sequence of similar and dissimilar tasks, Ke *et al.* [21] studied knowledge transfer by employing a complicated task similarity detection mechanism. Ke *et al.* [22] proposed a capsules and transfer routing method to improve knowledge transfer based on BERT. On the other hand, Lopez-Paz and Ranzato [32] proposed a gradient episodic memory method to minimize negative backward transfer. Lin *et al.* [28] proposed an orthogonal projection based method to modify the learned model of old tasks carefully for better backward knowledge transfer.

Besides addressing the issues of catastrophic forgetting and knowledge transfer, we also consider the robust generalization issue. To this end, we propose a new approach that prioritizes robust generalization in each task. This not only improves the model’s ability to perform well on the current task but also enhances its transferability to new tasks. Additionally, by encouraging the model to converge towards flatter local minima, we can reduce forgetting as well. Our approach can be easily combined with existing CL methods to further enhance their performance.

### 2.2. Robust Generalization

Solutions in robust generalization initially focused on increasing data diversity through augmentations [50, 9, 6, 13, 16, 17]. However, these works prioritize

either in-distribution generalization or out-of-distribution generalization but not both simultaneously. For instance, Cutout [9] improves in-distribution accuracy but not out-of-distribution robustness. AugMix [16] improves robustness but hurts accuracy. Later, researchers explored adversarial training to enhance out-of-distribution generalization [45, 47], but this often leads to compromised in-distribution generalization [43]. Lopes *et al.* [31] proposed a patch Gaussian augmentation scheme as an attempt towards robust generalization, but this approach only increases robustness to simple image corruptions, without significant accuracy gains.

Another line of research for robust generalization is shape and texture representation learning. Geirhos *et al.* [13] revealed that convolutional networks trained on natural images tend to learn texture representations that generalize well to in-distribution data but perform poorly on out-of-distribution data. To enhance the model’s out-of-distribution robustness, researchers have proposed shape representation learning methods [13, 17, 39], which often sacrifice in-distribution performance. Li *et al.* [26] propose shape-texture debiased training with a mixup loss to avoid bias towards either shape or texture, balancing in-distribution and out-of-distribution generalizations. However, this method underperforms in CL settings, as the mixup loss can hinder CL performance [35]. To address this issue, we propose a new online shape-texture self-distillation technique that enables learning both shape and texture representations for CL, leading to improved robust generalization. This approach avoids the use of a mixup loss and instead relies on self-distillation.

### 3. Method

#### 3.1. Problem setting

This paper focuses on the class-incremental scenario in CL, where the objective is to learn a unified classifier over incrementally occurring sets of classes [36]. Formally, let  $\mathcal{T} = \{\mathcal{T}_0, \dots, \mathcal{T}_T\}$  be a sequence of classification tasks,  $\mathcal{D}_t = \{(x_{i,t}, y_{i,t})\}_{i=0}^{n_t}$  be the labeled training set of the task  $\mathcal{T}_t$  with  $n_t$  samples from  $m_t$  distinct classes, and  $(x_{i,t}, y_{i,t})$  be the  $i$ -th (image, label) pair in the training set of the task  $\mathcal{T}_t$ . A single model  $\Theta$  is trained to solve the tasks  $\mathcal{T}$  incrementally. The model  $\Theta$  consists of a feature extractor and a unified classifier. For the initial task  $\mathcal{T}_0$ , the model  $\Theta_0$  learns a standard classifier for the first  $m_0$  classes. In the incremental step  $t$ , only the classifier is extended by adding  $m_t$  new output nodes to learn  $m_t$  new classes, leading to a new model  $\Theta_t$ . During the training of  $\Theta_t$ , only the training set  $\mathcal{D}_t$  for the task  $\mathcal{T}_t$  is available. In testing phase,  $\Theta_t$  is required to classify all classes seen so far, *i.e.*,  $\{m_0, \dots, m_t\}$ . This work emphasizes that  $\Theta_t$  should perform well on testing data, regardless of whether that data comes from the same

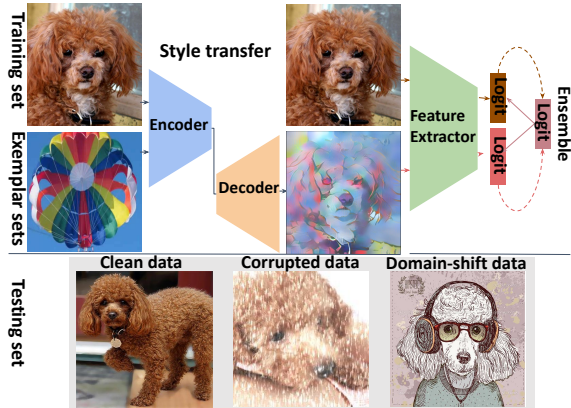


Figure 2: **Online shape-texture self-distillation (STSD).**

Given an image from the training set, we create its shape-texture conflict counterpart by transferring a different style from an image randomly sampled from exemplar sets. The original image and shape-texture conflict image are combined in the mini-batch for training, and their output logits are ensemble to create a new soft target for distillation, enabling the model to learn both shape and texture representations. Then the resulting model can effectively generalize to clean data, corrupted data, and domain-shifted data during inference.

*distribution as the training data or not.* Next, we introduce an new approach to achieve such robust generalization.

#### 3.2. Online shape-texture self-distillation

We propose a method to learn both shape and texture representations for each classification task, enabling generalization to both in-distribution and out-of-distribution data. While standard training on natural images tends to learn texture representations for in-distribution generalization, shape representations are more robust to distribution shifts. To encourage the model to learn shape representations, we adopt the approach of Geirhos *et al.* [13] by using shape-texture conflict images for training. However, we use styles from different images within the current training set  $\mathcal{D}_t$  rather than external artistic paintings, as storing paintings in memory is not feasible for memory-constrained CL. Specifically, during optimization at the incremental step  $t$ , we randomly sample two mini-batches of images with a size of  $k$  from the current training set  $\mathcal{D}_t$ . We use  $\mathcal{X} = \{x_{1,t}, \dots, x_{k,t}\}$  as content images and  $\hat{\mathcal{X}} = \{\hat{x}_{1,t}, \dots, \hat{x}_{k,t}\}$  as style images. We generate a mini-batch of shape-texture conflict images  $\tilde{\mathcal{X}} = \{\tilde{x}_{1,t}, \dots, \tilde{x}_{1,t}\}$  based on  $\mathcal{X}$  and  $\hat{\mathcal{X}}$ , where

$$\tilde{x}_{i,t} = f(x_{i,t}, \hat{x}_{i,t}). \quad (1)$$

Here  $f(\cdot)$  is the style transfer operation. In this paper, we use the real-time style transfer approach, AdaIN [19].

Training only on the original natural images tends to learn texture representations, while training only on shape-texture conflict images tends to learn shape representations. To learn both shape and texture representations simultaneously, we propose online shape-texture debiased self-distillation (STSD). Specifically, let  $\mathcal{X} = \{x_{1,t}, \dots, x_{k,t}\}$  be a mini-batch of images with a size of  $k$  randomly sampled from the current training set  $\mathcal{D}_t$  in the incremental step  $t$ , and  $\tilde{\mathcal{X}} = \{\tilde{x}_{1,t}, \dots, \tilde{x}_{k,t}\}$  be the corresponding mini-batch of shape-texture conflict images generated following **Eq. (1)**. Then we obtain a new mini-batch  $\{\mathcal{X}, \tilde{\mathcal{X}}\}$  by combining  $\mathcal{X}$  and  $\tilde{\mathcal{X}}$  for model training. Let  $\mathcal{Z} = \{z_{1,t}, \dots, z_{k,t}\}$  and  $\tilde{\mathcal{Z}} = \{\tilde{z}_{1,t}, \dots, \tilde{z}_{k,t}\}$  be the corresponding logit of  $\mathcal{X}$  and  $\tilde{\mathcal{X}}$ , produced by the model  $\Theta_t$ , respectively.  $\mathcal{Z}$  is generated using original natural images as input and is more likely to encode texture information. Conversely,  $\tilde{\mathcal{Z}}$  is generated using shape-texture conflict images as input, and is more likely to capture shape information.  $\mathcal{Z}$  and  $\tilde{\mathcal{Z}}$  are ensembled to integrate shape and texture knowledge. The resulting ensembled logit is then used as a soft target for distillation, which further enhances shape and texture representation learning. The distillation loss is defined by

$$\mathcal{L}^{STSD} = D_{KL}(p||q) + D_{KL}(\tilde{p}||q), \quad (2)$$

where  $p = \sigma(\mathcal{Z}/\tau)$ ,  $\tilde{p} = \sigma(\tilde{\mathcal{Z}}/\tau)$ ,  $q = \sigma((\mathcal{Z} + \tilde{\mathcal{Z}})/2\tau)$ .  $\tau$  is a temperature hyper-parameter,  $\sigma(\cdot)$  is a softmax function, and  $(\mathcal{Z} + \tilde{\mathcal{Z}})/2$  is the ensembled logit. Our distillation is developed from a mini-batch in an online manner, which only requires minimal computations without the need of introducing extra network parameters.

### 3.3. Adaption to exemplar replay

We adopt exemplar replay, a popular approach to mitigate forgetting, and enhance its effectiveness by incorporating our approach. Specifically, instead of using the styles from the current training set, we use the styles from images in the exemplar sets to generate shape-texture conflict images as the exemplar sets contain a larger variety of classes and introduce more diverse styles. Additionally, we do not perform online shape-texture self-distillation during replay to prevent the introduction of noise from low-quality synthesized shape-texture conflict images. Empirical evidence (see **Sec. 4.5**) supports our approach to replay only with original natural images from the exemplar sets, which reduces the harmful effects of noise and improves performance. Our proposed CL approach is illustrated in **Fig. 2**, and its implementation is outlined in **Algorithm 1**. At each incremental step  $t$ , the overall loss function is defined as:

$$\mathcal{L}_t = \mathcal{L}_{\mathcal{D}_t, \tilde{\mathcal{D}}_t}^{CE} + \mathcal{L}_{\mathcal{P}}^{CE} + \gamma \mathcal{L}_{\mathcal{D}_t, \tilde{\mathcal{D}}_t}^{STSD}, \quad (3)$$

where cross-entropy loss  $\mathcal{L}_{\mathcal{D}_t, \tilde{\mathcal{D}}_t}^{CE}$  is computed on the combination of shape-texture conflict images  $\mathcal{D}_t$  and the

original natural images  $\tilde{\mathcal{D}}_t$  from the current task  $t$ . For the replay,  $\mathcal{L}_{\mathcal{P}}^{CE}$  is computed only on the original natural images from exemplar sets  $\mathcal{P}$ . The last item is the proposed STSD loss, and  $\gamma$  is a constant used to control its strength.

---

#### Algorithm 1: CL with robust generalization

---

**input:**  $\mathcal{D}_t$ ; /\*the training set for the new task \*/  
**require:**  $\mathcal{P} = \{\mathcal{P}_i\}_{i=0}^{t-1}$ ; /\*the current exemplar sets for replay\*/  
**require:**  $f$ ; /\*the style transfer model\*/  
**output:**  $\Theta_t$ ; /\*the new model to be learned from the new task\*/

- 1  $\Theta_t \leftarrow \Theta_{t-1}$ ; /\*add  $m_t$  new output nodes\*/
- 2 construct new exemplar set  $\mathcal{P}_t$ ;
- 3  $\mathcal{P} \leftarrow \{\mathcal{P}_i\}_{i=0}^{t-1} \cup \mathcal{P}_t$ ; /\*add  $\mathcal{P}_t$  to replay buffer\*/
- 4 **for** iteration  $j \leftarrow 1$  **to**  $l$  **do**
- 5     load a mini-batch  $(\mathcal{X}_t, \mathcal{Y}_t)$  from  $\mathcal{D}_t$ ;
- 6      $\mathcal{X}_t \leftarrow \{(x_{i,t})\}_{i=1}^k$ ;  $\mathcal{Y}_t \leftarrow \{(y_{i,t})\}_{i=1}^k$ ;
- 7     load a mini-batch  $(\hat{\mathcal{X}}_t, \hat{\mathcal{Y}}_t)$  from  $\mathcal{P}$ ;
- 8      $\hat{\mathcal{X}}_t \leftarrow \{(\hat{x}_{i,t})\}_{i=1}^k$ ;  $\hat{\mathcal{Y}}_t \leftarrow \{(\hat{y}_{i,t})\}_{i=1}^k$ ;
- 9      $\tilde{\mathcal{X}}_t \leftarrow \{f(x_{i,t}, \hat{x}_{i,t})\}_{i=1}^k$ ; /\*using Eq.(1)\*/
- 10     $\mathcal{Z}_t, \tilde{\mathcal{Z}}_t \leftarrow \Theta_t(\mathcal{X}_t, \tilde{\mathcal{X}}_t)$ ; /\*forward pass for new task\*/
- 11    Compute  $\mathcal{L}_{\mathcal{D}_t, \tilde{\mathcal{D}}_t}^{STSD}$  with  $(\mathcal{Z}_t, \tilde{\mathcal{Z}}_t)$  using Eq.(2);
- 12    Compute  $\mathcal{L}_{\mathcal{D}_t, \tilde{\mathcal{D}}_t}^{CE}$  with  $\{(\mathcal{Z}_t, \mathcal{Y}_t), (\tilde{\mathcal{Z}}_t, \mathcal{Y}_t)\}$ ;
- 13     $\hat{\mathcal{Z}}_t \leftarrow \Theta_t(\hat{\mathcal{X}}_t)$ ; /\*forward pass for replay\*/
- 14    Compute  $\mathcal{L}_{\mathcal{P}}^{CE}$  with  $(\hat{\mathcal{Z}}_t, \hat{\mathcal{Y}}_t)$ ;
- 15     $\mathcal{L}_t = \mathcal{L}_{\mathcal{D}_t, \tilde{\mathcal{D}}_t}^{CE} + \mathcal{L}_{\mathcal{P}}^{CE} + \gamma \mathcal{L}_{\mathcal{D}_t, \tilde{\mathcal{D}}_t}^{STSD}$  optimize  $\Theta_t$  with loss  $\mathcal{L}_t$ ; /\*backward pass\*/

---

## 4. Experiments and results

### 4.1. Experimental setup

**Datasets.** We perform class-incremental experiments on three standard datasets including CIFAR-100 [24], ImageNet-100, and ImageNet-1000 [8], following, e.g., [18, 30, 42, 12]. ImageNet-100 is a subset of Imagenet-1000 with 100 classes that are randomly sampled using the NumPy seed of 1993. We use the dataset ImageNet-1000-C [1], CIFAR-100-C [1], and ImageNet-1000-R [15] for evaluating out-of-distribution generalization. ImageNet-1000-C and CIFAR-100-C consist of 15 diverse corruption types applied to validation images of ImageNet-1000 and CIFAR-100, respectively, with five different severity levels for each corruption type. ImageNet-1000-R is a real-world distribution shift dataset that includes changes in image style, geographic location, etc. We made ImageNet-100-C and ImageNet-100-R from ImageNet-1000-C and ImageNet-1000-R using the same procedure as for ImageNet-100 from ImageNet-1000.

**Protocols.** We follow the protocol proposed in [18], which has been adopted in many recent works [18, 30, 42,



11, 35, 12], to simulate practical class-incremental learning. The protocol consists of an initial base task  $\mathcal{T}_0$  followed by  $T$  incremental tasks, where  $T$  is set to 5 or 10. For all datasets, we assign half of the classes to the initial base task and distribute the remaining classes equally over the incremental steps. Additionally, we allow only 20 exemplars for each class to be saved for replay.

**Metrics.** We report the experimental results with six different metrics. Different from previous works in CL, we define CL performance in terms of all the six metrics below. An ideal system with outstanding CL performance would have high **Acc.**, **FWT**, **BWT**, and  **$\mathcal{R}$ -**R**** and, low  **$\mathcal{F}$**  and  **$\mathcal{R}$ -**C****.

Specifically, average incremental accuracy (**Acc.**) [36] is computed by averaging the accuracies of the models  $\{\Theta_0, \dots, \Theta_T\}$  obtained in incremental steps. Each model’s accuracy is evaluated on all classes seen thus far. Forgetting rate ( **$\mathcal{F}$** ) [30] measures the performance drop on the initial base task  $\mathcal{T}_0$ . It is the gap between the accuracy of  $\Theta_0$  and the accuracy of  $\Theta_T$  on the same testing data of  $\mathcal{T}_0$ . To assess knowledge transfer, we use forward knowledge transfer (**FWT**) [32], which measures the mean difference in accuracy between tasks trained continuously and those trained from scratch, across all tasks. Similarly, we use backward knowledge transfer (**BWT**) [32] to measure the average accuracy change of each task after learning new tasks. The robustness of the final model  $\Theta_T$  against data corruptions ( **$\mathcal{R}$ -**C****) [1] is measured by computing mean corruption error on ImageNet-100-C, ImageNet-1000-C and CIFAR-100-C. The robustness of the final model  $\Theta_T$  against domain shifts ( **$\mathcal{R}$ -**R****) [15] is measured by computing accuracy on ImageNet-100-R and ImageNet-1000-R.

**Implementation details.** The experiments are conducted based on the publicly available official code provided by Mittal *et al.* [35]. For ImageNet-100 and ImageNet-1000, we use an 18-layer ResNet. The network is trained for 70 epochs in the initial base task with a base learning rate of 1e-1, and is trained for 40 epochs in the incremental task with a base learning rate of 1e-2. The base learning rate is divided by 10 at epochs  $\{30, 60\}$  in the initial base task, and is divided by 10 at epochs  $\{25, 35\}$  in the incremental steps. For CIFAR-100, we use a 32-layer ResNet. The network is trained for 120 epochs in the initial base task with a base learning rate of 1e-1, and is trained for 60 epochs in the subsequent incremental tasks with a base learning rate of 1e-2. We adopt a cosine learning rate schedule, in which the learning rate is decayed until 1e-4. For all networks, the last layer is cosine normalized, as suggested in [18]. All networks are optimized using the SGD optimizer with a mini-batch of 128, a momentum of 0.9, and a weight decay of 1e-4. Following [18, 35], we use an adaptive weighting function for knowledge distillation loss. For each incremental step  $t$ ,  $\lambda_t = \lambda_{base} (\sum_{i=0}^t m_i / m_t)^{2/3}$  where  $\sum_{i=0}^t m_i$  denotes the number of all seen classes from step

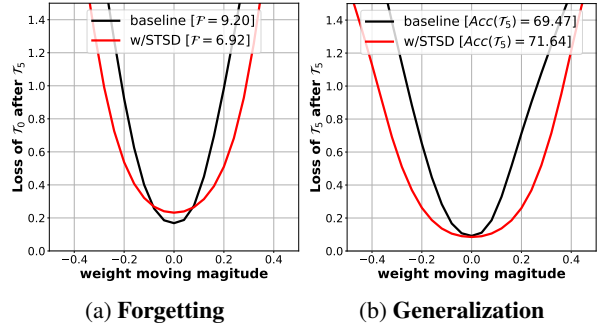


Figure 3: **Flatter local minima.** (a) is the weight loss landscape of the initial task  $\mathcal{T}_0$  after learning the fifth task  $\mathcal{T}_5$ . STSD finds flatter local minima than baseline, which explains why our approach helps to reduce forgetting from  $\mathcal{F} = 9.20$  to  $\mathcal{F} = 6.92$ ; (b) is the weight loss landscape of the fifth task  $\mathcal{T}_5$  after just learning the fifth task  $\mathcal{T}_5$ . STSD helps to improve the accuracy of  $\mathcal{T}_5$  from 69.47 to 71.64 by widening the local minima.

0 to step  $t$ , and  $m_t$  denotes the number of classes in step  $t$ .  $\lambda_{base}$  is set to 20 for CIFAR-100, 100 for ImageNet-100, and 600 for ImageNet-1000, as suggested by [35].  $\gamma$  is set to 0.01 by default. All codes will be made publicly available.

## 4.2. Benefits of robust generalization in generic CL

The majority of CL methods are developed based on two key generic components: replay and knowledge distillation. In this experiment, we aim to study whether STSD can be effectively applied in generic CL frameworks. In the next subsection, we will narrow down to specific CL methods and examine the effectiveness of STSD in combination with these CL methods.

**Generic CL frameworks.** Our experiments are conducted on ImageNet-100 with  $T=5$  and  $T=10$ , and four generic CL approaches: 1) *Naive* trains the model on the sequence of tasks without any measures to prevent forgetting. To prevent forgetting, 2) *w/Replay* employs exemplar replay, 3) *w/KD* uses knowledge distillation, and 4) *w/Replay+KD* uses both exemplar replay and knowledge distillation. All approaches follow the implementation details outlined in **Sec. 4.1**. We present the results in **Table 1**, comparing the outcomes obtained by utilizing the proposed STSD to those obtained without it.

**Result analysis.** Table 1 (a) demonstrates that the proposed STSD improves both out-of-distribution generalization ( **$\mathcal{R}$ -**C**** and  **$\mathcal{R}$ -**R****) and in-distribution generalization (**Acc.**) across protocols and baselines. The benefits of STSD are more pronounced when used in conjunction with generic CL frameworks, originally designed for preventing catastrophic forgetting. For instance, STSD reduces  **$\mathcal{R}$ -**C**** by 9.75 and 19.57 for *Naive* and *w/Replay+KD*, respectively, when  $T=5$ . In Table 1 (b), we show that using STSD consistently results in

	Naive			w/ Replay			w/ KD			w/ Replay+KD		
	$R-C\downarrow$	$R-R\uparrow$	Acc. $\uparrow$	$R-C\downarrow$	$R-R\uparrow$	Acc. $\uparrow$	$R-C\downarrow$	$R-R\uparrow$	Acc. $\uparrow$	$R-C\downarrow$	$R-R\uparrow$	Acc. $\uparrow$
w/o STSD ( $T=5$ )	116.43	19.46	56.80	99.69	21.98	68.29	94.49	19.53	68.55	87.16	26.66	76.55
w/ STSD ( $T=5$ )	<b>106.68</b>	<b>26.92</b>	<b>58.64</b>	<b>88.79</b>	<b>30.60</b>	<b>69.51</b>	<b>82.21</b>	<b>29.01</b>	<b>70.83</b>	<b>67.59</b>	<b>39.53</b>	<b>78.76</b>
w/o STSD ( $T=10$ )	120.71	16.51	51.16	102.62	19.99	64.69	99.47	15.72	63.23	90.97	23.84	74.76
w/ STSD ( $T=10$ )	<b>114.54</b>	<b>21.45</b>	<b>53.94</b>	<b>95.88</b>	<b>29.34</b>	<b>65.89</b>	<b>90.92</b>	<b>23.47</b>	<b>64.70</b>	<b>74.87</b>	<b>35.11</b>	<b>76.25</b>

(a) Robust generalization: out-of-distribution generalization ( $\mathcal{R}-C$  and  $\mathcal{R}-R$ ) and in-distribution generalization(Acc.)

	Naive			w/ Replay			w/KD			w/ Replay+KD		
	FWT $\uparrow$	BWT $\uparrow$	$\mathcal{F}\downarrow$	FWT $\uparrow$	BWT $\uparrow$	$\mathcal{F}\downarrow$	FWT $\uparrow$	BWT $\uparrow$	$\mathcal{F}\downarrow$	FWT $\uparrow$	BWT $\uparrow$	$\mathcal{F}\downarrow$
w/o STSD ( $T=5$ )	3.28	-56.24	50.12	2.20	-22.03	29.56	1.56	-3.88	4.58	1.08	-6.76	9.20
w/ STSD ( $T=5$ )	<b>4.56</b>	<b>-50.68</b>	<b>45.44</b>	<b>3.80</b>	<b>-19.88</b>	<b>25.84</b>	<b>3.76</b>	<b>-2.06</b>	<b>3.44</b>	<b>3.16</b>	<b>-4.58</b>	<b>6.92</b>
w/o STSD ( $T=10$ )	3.92	-55.56	50.00	3.28	-24.28	31.68	2.64	-3.52	3.80	2.80	-7.71	16.32
w/ STSD ( $T=10$ )	<b>4.76</b>	<b>-52.93</b>	<b>44.16</b>	<b>4.20</b>	<b>-22.23</b>	<b>27.92</b>	<b>4.00</b>	<b>-2.86</b>	<b>3.04</b>	<b>3.60</b>	<b>-6.61</b>	<b>13.32</b>

(b) Better transfer and less forgetting: forward knowledge transfer (FWT), backward knowledge transfer(BWT), forgetting ( $\mathcal{F}$ )

Table 1: **Our STSD is adaptable to and effective in generic CL frameworks** Benefits analysis on ImageNet-100 with  $T=5$  and  $T=10$ . Robust generalization is improved by using the proposed STSD across four CL genetic approaches, including *Naive*, *w/ Replay*, *w/ KD*, *w/ Replay+KD*. Improved robust generalization also leads to better knowledge transfer and less forgetting.

higher FWT and lower negative BWT across protocols and baselines. Higher FWT and lower negative BWT indicate better learning of new tasks and less forgetting (lower  $\mathcal{F}$ ), respectively.

**Flatness of local minima.** One reason for exploring robust generalization in CL is that striving for it can result in flatter local minima, which in turn can lead to better generalization and less forgetting. The benefits of using the proposed STSD to achieve robust generalization in CL are demonstrated in Table 1. To investigate whether STSD leads to flatter local minima, we visualize the weight loss landscape produced with or without STSD, based on the baseline *w/ Replay+KD* in the setting of  $T=5$ . To do this, we adopt the visualization method proposed by Li *et al.* [25]. We randomly select a direction and move the weights of the network in that direction with a given magnitude, then plot the changes in its training loss. We perform this visualization five times and present the average result.

We start by analyzing the forgetting of the networks by visualizing changes in the weight loss landscape for  $\mathcal{T}_0$  after  $\mathcal{T}_5$ . Figure 3a shows that STSD leads to the discovery of a flatter local minimum, resulting in less forgetting. We then investigate the generalization of the networks by examining the performance of  $\mathcal{T}_5$  immediately after learning it. As depicted in Figure 3b, STSD again leads to the discovery of a flatter loss minimum, resulting in higher accuracy. Therefore, these results suggest that achieving robust generalization using STSD tends to find flatter local minima, resulting in better generalization and less forgetting.

### 4.3. Connecting to the state-of-the-art in CL

In the previous subsection, we demonstrate that our STSD is adaptable to generic CL frameworks. Here, our goal

is to show that our STSD can be seamlessly integrated with state-of-the-art CL methods to achieve even better performances.

**SOTA baselines in CL.** Specifically, we combine our STSD with three recent SOTA CL approaches: CCIL [35], Podnet [11], and AFC [20]. We implement these approaches and incorporate our STSD into the publicly available official code provided by each approach.

**Result analysis.** In Table 2, we present our results on three datasets and two protocols. Our approach consistently outperforms the baselines in terms of generalization, forgetting, and robustness. For instance, when applied to AFC on ImageNet-100 with  $T=5$ , our approach increases the accuracy from 78.68 to 80.83 and decreases the forgetting metric  $\mathcal{F}$  from 3.51 to 1.35. Moreover, our approach reduces  $R-C$  by 16.7 and improves  $R-R$  by 10.31, demonstrating its effectiveness in enhancing the robustness of these state-of-the-art methods.

### 4.4. Comparison to robust generalization baselines

Achieving robust generalization remains a challenging task (Sec.2). To assess the performance of competitive robust generalization methods and our STSD, we fix the CL framework (with replay and knowledge distillation), combine robust generalization methods with this backbone, and compare their CL performance.

**Robust generalization baselines.** We compare the different robust generalization baselines that can facilitate shape-texture representation learning. As control experiments, we fix the same CL framework *w/ Replay+KD* and combine the following set of robust generalization baselines with *w/ Replay+KD*. Here is a list of the baselines: 1) *standard*: This baseline doesn't use any techniques to

	ImageNet-100				ImageNet-1000				CIFAR-100		
	$R-C\downarrow$	$R-R\uparrow$	Acc. $\uparrow$	$\mathcal{F}\downarrow$	$R-C\downarrow$	$R-R\uparrow$	Acc. $\uparrow$	$\mathcal{F}\downarrow$	$R-C\downarrow$	Acc. $\uparrow$	$\mathcal{F}\downarrow$
CCIL[35] ( $T=5$ )	86.02	25.8	77.03	12.88	74.19	15.64	67.46	12.94	67.38	64.33	18.36
CCIL + STSD ( $T=5$ , <i>ours</i> )	<b>69.74</b>	<b>40.12</b>	<b>79.16</b>	<b>7.80</b>	<b>69.12</b>	<b>19.66</b>	<b>67.84</b>	<b>10.92</b>	<b>62.81</b>	<b>65.13</b>	<b>13.64</b>
Podnet [11] ( $T=5$ )	113.19	20.72	77.95	6.05	87.19	10.40	68.76	7.89	67.21	65.08	11.68
Podnet + STSD ( $T=5$ , <i>ours</i> )	<b>100.64</b>	<b>27.19</b>	<b>78.45</b>	<b>4.72</b>	<b>81.42</b>	<b>13.82</b>	<b>69.13</b>	<b>7.28</b>	<b>66.52</b>	<b>65.93</b>	<b>9.36</b>
AFC [20] ( $T=5$ )	110.53	18.44	78.68	3.51	86.74	10.37	68.75	6.85	66.83	65.80	8.17
AFC + STSD ( $T=5$ , <i>ours</i> )	<b>93.83</b>	<b>28.75</b>	<b>80.83</b>	<b>1.35</b>	<b>81.24</b>	<b>14.72</b>	<b>69.48</b>	<b>5.70</b>	<b>65.66</b>	<b>66.07</b>	<b>6.55</b>
CCIL[35] ( $T=10$ )	92.96	23.71	74.25	16.12	76.31	14.31	65.20	17.46	70.07	63.01	21.06
CCIL + STSD ( $T=10$ , <i>ours</i> )	<b>75.45</b>	<b>34.58</b>	<b>76.72</b>	<b>12.60</b>	<b>71.92</b>	<b>17.84</b>	<b>66.47</b>	<b>14.31</b>	<b>63.83</b>	<b>63.69</b>	<b>15.94</b>
Podnet[35] ( $T=10$ )	116.50	19.73	75.31	18.07	88.72	8.99	65.98	15.77	68.86	63.20	22.39
Podnet + STSD ( $T=10$ , <i>ours</i> )	<b>103.00</b>	<b>26.72</b>	<b>76.11</b>	<b>16.41</b>	<b>82.41</b>	<b>12.85</b>	<b>66.32</b>	<b>15.50</b>	<b>66.99</b>	<b>63.69</b>	<b>18.13</b>
AFC [20] ( $T=10$ )	112.38	19.43	76.97	13.8	89.16	7.91	67.03	13.44	68.21	64.18	16.26
AFC + STSD ( $T=10$ , <i>ours</i> )	<b>95.63</b>	<b>25.80</b>	<b>79.15</b>	<b>12.07</b>	<b>82.67</b>	<b>12.03</b>	<b>68.25</b>	<b>12.63</b>	<b>67.79</b>	<b>64.95</b>	<b>12.95</b>

Table 2: **The State-Of-The-Art (SOTA) CL methods combined with our STSD yield significantly better CL performance than SOTA alone**. Our approach can be readily combined with the state of the art to further reduce forgetting ( $\mathcal{F}$ ), and boost robustness against out-of-distribution ( $\mathcal{R}-C$  and  $\mathcal{R}-R$ ) considerably across protocols and datasets.

encourage learning both shape and texture representations; 2) *augmentation*: This baseline follows Hermann *et al.* [17] to enhance shape representation learning by applying simple, naturalistic augmentations such as color distortion, noise, and blur. Specifically, we use the color jitter with a probability of 80%, the color drop with a probability of 20%, Gaussian noise (mean=0 and std=0.025) with a probability of 50%, and Gaussian blur (kernel size is 10% of the image width/height) with a probability of 50%, as specified by [17]; 3) *painting-style*: This baseline follows Geirhos *et al.* [13] to generate shape-texture conflict images using the styles from artistic paintings, which requires additional memory to store the paintings. This baseline trains the models jointly on both shape-texture conflict images and original natural images; 4) *mixup-loss*: This baseline follows Li *et al.* [26] to generate shape-texture conflict images by style transfer using AdaIN, where the used styles are from the current training set. This baseline also trains the models jointly on both shape-texture conflict images and original natural images. Additionally, it provides a mixup loss (refer to Eq. (1) in [26]) for shape-texture conflict images, where  $\lambda$  is set to 0.8 as suggested. 5) *no-loss*: This baseline generates shape-texture conflict images following the same manner as STSD and trains the models jointly on both shape-texture conflict images and original natural images, but without using the STSD loss (defined in Eq. 2).

**Result analysis.** The results on ImageNet-100 with  $T=5$  are presented in Figure 4. The following main observations can be made: 1) All methods surpass *standard* in terms of out-of-distribution generalization. Notably, our STSD approach yields the best results in this regard; 2) Our STSD exhibit significant improvements in in-distribution generalization, whereas the *augmentation* and *painting-style* methods show weaker in-distribution generalization performance than the standard. This indicates that although these techniques enhance out-of-distribution

generalization, they come at the cost of sacrificing in-distribution generalization; 3) All methods reduce forgetting compared to the standard. This finding implies that improving out-of-distribution generalization is critical for mitigating forgetting in CL, as it enables the model to find flatter local minima [41]. Notably, *mixup-loss* performs even worse than *augmentation* and *painting-style* in reducing forgetting, highlighting that mixup loss is not a suitable technique for CL, consistent with [35].

#### 4.5. Ablation studies and further analysis

To evaluate the contribution of each individual component in our STSD, we repeat the experiments on ImageNet-100 using the ablated versions of our method. We also analyze more benefits that our STSD can bring to CL.

**The effect of coefficient  $\gamma$ .** We conducted an empirical study to analyze the effect of the coefficient  $\gamma$  in the overall loss function in Eq. 3, which controls the strength of the STSD. Specifically, we considered four different settings of  $\gamma \in \{0, 0.001, 0.01, 0.1\}$  and evaluated their performance on various metrics, where STSD is not used when  $\gamma$  is set to 0. The results, presented in Table 3, demonstrate that incorporating STSD with  $\gamma \in 0.001, 0.01, 0.1$  leads to improved performance compared to the case when  $\gamma=0$ , across all metrics. This suggests that the STSD is essential for enhancing the model’s performance. We also observed that higher values of  $\gamma$  lead to less forgetting but may deteriorate robust generalization. By setting a suitable value of  $\gamma$  (e.g.,  $\gamma=0.01$ ), we achieved a good overall performance across all metrics.

**Styles from exemplar sets vs. current training set.** In Section 3.3, we proposed using the styles from exemplar sets instead of the current training set to generate shape-texture conflict images when exemplars are available for replay. Exemplar sets offer more diverse styles than the current training set, making them a better choice. We conducted

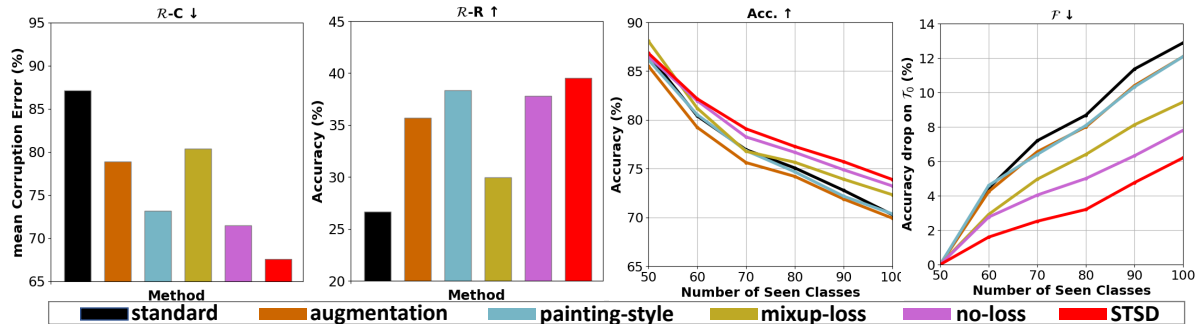


Figure 4: **Our STSD is superior to all the compared baselines in improving robust generalization and reducing forgetting on ImageNet-100 with  $T=5$ .**

	$R-C \downarrow$	$R-R \uparrow$	$Acc. \uparrow$	$\mathcal{F} \downarrow$
$\gamma=0$	87.16	26.66	76.55	9.20
$\gamma=0.001$	68.86	38.12	77.97	8.32
$\gamma=0.01$	<b>67.59</b>	<b>39.53</b>	<b>78.76</b>	6.92
$\gamma=0.1$	68.98	39.19	77.89	<b>6.52</b>

Table 3: **Sensitivity analysis on coefficient  $\gamma$  on ImageNet-100 with  $T=5$ .**

an empirical comparison to validate this hypothesis. The results in Table 4 support our hypothesis that using styles from exemplar sets leads to better performance across all metrics compared to using styles from the current data.

	$R-C \downarrow$	$R-R \uparrow$	$Acc. \uparrow$	$\mathcal{F} \downarrow$
Current training set	70.70	38.83	77.86	8.44
Exemplar sets	<b>67.59</b>	<b>39.53</b>	<b>78.76</b>	<b>6.92</b>

Table 4: **Styles from exemplar sets is better than from current training sets on ImageNet-100 with  $T=5$ .**

**STSD used in replay?** We investigate the impact of STSD in replay and present our findings in Table 5. As described in Section 3.3, we proposed fine-tuning with only the original natural images in exemplar sets to mitigate the negative impact of noise from shape-texture conflict images. The experimental results confirm that incorporating STSD in replay does not yield better performance.

	$R-C \downarrow$	$R-R \uparrow$	$Acc. \uparrow$	$\mathcal{F} \downarrow$
Yes	69.68	38.45	77.58	7.95
No	<b>67.59</b>	<b>39.53</b>	<b>78.76</b>	<b>6.92</b>

Table 5: **Using STSD in replay is unfavorable on ImageNet-100 with  $T=5$ .**

**Longer Task Sequence.** We conducted additional experiments on ImageNet-100 to evaluate the effectiveness of the proposed STSD with  $T=25$  and  $T=50$ . We utilized the baseline CCIL [35] and report the results in Table 6. The results demonstrate that STSD is still able to effectively improve the performance of existing CL methods like CCIL even for a much larger number of tasks across metrics.

**Connecting to vision transformer.** We assessed the impact of STSD on newly emerged vision transformer

	$R-C \downarrow$	$R-R \uparrow$	$Acc. \uparrow$	$\mathcal{F} \downarrow$
CCIL [35] ( $T=25$ )	99.13	20.62	67.47	22.84
w/ STSD ( $T=25$ , <i>ours</i> )	<b>85.43</b>	<b>29.74</b>	<b>70.29</b>	<b>20.08</b>
CCIL [35] ( $T=50$ )	106.10	16.91	59.15	34.04
w/ STSD ( $T=50$ , <i>ours</i> )	<b>98.40</b>	<b>22.48</b>	<b>62.16</b>	<b>31.76</b>

Table 6: **STSD improves CL performance on longer task sequences on ImageNet-100 with  $T=25$  and  $T=50$ .**

architecture [10]. Yu *et al.* [48] proposed a recipe to use vision transformers for CL, and we incorporated STSD into this recipe. We followed their implementation details. Our findings from Table 7 demonstrate that using STSD improves performance across various metrics, consistent with the results obtained from the convolutional neural network (CNN)-based CL approaches such as CCIL [35]. However, we observed that the improvements achieved by STSD when using vision transformers were relatively lower than those obtained through CNNs. This may be attributed to the fact that vision transformers have already learned better shape and texture representations than CNNs [44].

	$R-C \downarrow$	$R-R \uparrow$	$Acc. \uparrow$	$\mathcal{F} \downarrow$
ViTIL [48]	82.36	34.54	78.17	6.56
w/ STSD ( <i>ours</i> )	<b>76.75</b>	<b>38.42</b>	<b>78.71</b>	<b>5.12</b>
CCIL [35]	86.02	25.80	77.03	12.88
w/ STSD ( <i>ours</i> )	<b>69.74</b>	<b>40.12</b>	<b>79.16</b>	<b>7.80</b>

Table 7: **STSD is consistently improves performance regardless of architectures on ImageNet-100 with  $T=5$ .**

## 5. Conclusion

We have tackled the challenging problem of CL with the objectives of accumulating knowledge, transferring knowledge across tasks, and generalizing over unseen data regardless of its distribution. To achieve these objectives simultaneously, we proposed a novel online shape-texture self-distillation (STSD) method that learns both shape and texture representations for each task, aiming to achieve robust generalization in CL. Our approach can be easily integrated with existing CL methods and improves generalization, encourages knowledge transfer, and reduces forgetting.



## References

- [1] *Benchmarking neural network robustness to common corruptions and perturbations*, 2019. 4, 5
- [2] Rahaf Aljundi, Francesca Babiloni, Mohamed Elhoseiny, Marcus Rohrbach, and Tinne Tuytelaars. Memory aware synapses: Learning what (not) to forget. In *ECCV*, 2018. 2
- [3] Francisco M Castro, Manuel J Marín-Jiménez, Nicolás Guil, Cordelia Schmid, and Karteek Alahari. End-to-end incremental learning. In *ECCV*, 2018. 2
- [4] Sungmin Cha, Hsiang Hsu, Taebaek Hwang, Flavio P Calmon, and Taesup Moon. Cpr: classifier-projection regularization for continual learning. In *ICLR*, 2021. 2
- [5] Arslan Chaudhry, Jiefeng Chen, Timothy Nguyen, and Gorur Dilan. Is forgetting less a good inductive bias for forward transfer? In *ICLR*, 2023. 2
- [6] Ekin D Cubuk, Barret Zoph, Dandelion Mane, Vijay Vasudevan, and Quoc V Le. Autoaugment: Learning augmentation policies from data. *arXiv preprint arXiv:1805.09501*, 2018. 2
- [7] Danruo Deng, Guangyong Chen, Jianye Hao, Qiong Wang, and Pheng-Ann Heng. Flattening sharpness for dynamic gradient projection memory benefits continual learning. In *NeurIPS*, 2021. 2
- [8] Jia Deng, Wei Dong, Richard Socher, Li-Jia Li, Kai Li, and Li Fei-Fei. Imagenet: A large-scale hierarchical image database. In *CVPR*, 2009. 4
- [9] Terrance DeVries and Graham W Taylor. Improved regularization of convolutional neural networks with cutout. *arXiv preprint arXiv:1708.04552*, 2017. 2, 3
- [10] Alexey Dosovitskiy, Lucas Beyer, Alexander Kolesnikov, Dirk Weissenborn, Xiaohua Zhai, Thomas Unterthiner, Mostafa Dehghani, Matthias Minderer, Georg Heigold, Sylvain Gelly, et al. An image is worth 16x16 words: Transformers for image recognition at scale. In *ICLR*, 2021. 8
- [11] Arthur Douillard, Matthieu Cord, Charles Ollion, Thomas Robert, and Eduardo Valle. Podnet: Pooled outputs distillation for small-tasks incremental learning. In *ECCV*, 2020. 2, 5, 6, 7
- [12] Arthur Douillard, Alexandre Ramé, Guillaume Couairon, and Matthieu Cord. Dytox: Transformers for continual learning with dynamic token expansion. In *CVPR*, 2022. 4, 5
- [13] Robert Geirhos, Patricia Rubisch, Claudio Michaelis, Matthias Bethge, Felix A Wichmann, and Wieland Brendel. Imagenet-trained cnns are biased towards texture; increasing shape bias improves accuracy and robustness. *arXiv preprint arXiv:1811.12231*, 2018. 2, 3, 7
- [14] Ian J Goodfellow, Mehdi Mirza, Da Xiao, Aaron Courville, and Yoshua Bengio. An empirical investigation of catastrophic forgetting in gradient-based neural networks. *arXiv preprint arXiv:1312.6211*, 2013. 2
- [15] Dan Hendrycks, Steven Basart, Norman Mu, Saurav Kadavath, Frank Wang, Evan Dorundo, Rahul Desai, Tyler Zhu, Samyak Parajuli, Mike Guo, et al. The many faces of robustness: A critical analysis of out-of-distribution generalization. In *ICCV*, 2021. 4, 5
- [16] Dan Hendrycks, Norman Mu, Ekin D Cubuk, Barret Zoph, Justin Gilmer, and Balaji Lakshminarayanan. Augmix: A simple data processing method to improve robustness and uncertainty. *arXiv preprint arXiv:1912.02781*, 2019. 2, 3
- [17] Katherine Hermann, Ting Chen, and Simon Kornblith. The origins and prevalence of texture bias in convolutional neural networks. In *NeurIPS*, 2020. 2, 3, 7
- [18] Saihui Hou, Xinyu Pan, Chen Change Loy, Zilei Wang, and Dahua Lin. Learning a unified classifier incrementally via rebalancing. In *CVPR*, 2019. 2, 4, 5
- [19] Xun Huang and Serge Belongie. Arbitrary style transfer in real-time with adaptive instance normalization. In *ICCV*, 2017. 3
- [20] Minsoo Kang, Jaeyoo Park, and Bohyung Han. Class-incremental learning by knowledge distillation with adaptive feature consolidation. In *CVPR*, 2022. 6, 7
- [21] Zixuan Ke, Bing Liu, and Xingchang Huang. Continual learning of a mixed sequence of similar and dissimilar tasks. In *NeurIPS*, 2020. 2
- [22] Zixuan Ke, Bing Liu, Nianzu Ma, Hu Xu, and Lei Shu. Achieving forgetting prevention and knowledge transfer in continual learning. In *NeurIPS*, 2021. 2
- [23] James Kirkpatrick, Razvan Pascanu, Neil Rabinowitz, Joel Veness, Guillaume Desjardins, Andrei A Rusu, Kieran Milan, John Quan, Tiago Ramalho, Agnieszka Grabska-Barwinska, et al. Overcoming catastrophic forgetting in neural networks. *Proceedings of the national academy of sciences*, 114(13):3521–3526, 2017. 2
- [24] Alex Krizhevsky, Geoffrey Hinton, et al. Learning multiple layers of features from tiny images. 2009. 4
- [25] Hao Li, Zheng Xu, Gavin Taylor, Christoph Studer, and Tom Goldstein. Visualizing the loss landscape of neural nets. In *NeurIPS*, 2018. 6
- [26] Yingwei Li, Qihang Yu, Mingxing Tan, Jieru Mei, Peng Tang, Wei Shen, Alan Yuille, and Cihang Xie. Shape-texture debiased neural network training. In *ICLR*, 2021. 2, 3, 7
- [27] Zhizhong Li and Derek Hoiem. Learning without forgetting. *IEEE TPAMI*, 40(12):2935–2947, 2017. 2
- [28] Sen Lin, Li Yang, Deliang Fan, and Junshan Zhang. Beyond not-forgetting: Continual learning with backward knowledge transfer. In *NeurIPS*, 2022. 2
- [29] Sen Lin, Li Yang, Deliang Fan, and Junshan Zhang. Trgp: Trust region gradient projection for continual learning. In *ICLR*, 2022. 2
- [30] Yaoyao Liu, Yuting Su, An-An Liu, Bernt Schiele, and Qianru Sun. Mnemonics training: Multi-class incremental learning without forgetting. In *CVPR*, 2020. 2, 4, 5
- [31] Raphael Gontijo Lopes, Dong Yin, Ben Poole, Justin Gilmer, and Ekin D Cubuk. Improving robustness without sacrificing accuracy with patch gaussian augmentation. *arXiv preprint arXiv:1906.02611*, 2019. 2, 3
- [32] David Lopez-Paz and Marc’Aurelio Ranzato. Gradient episodic memory for continual learning. In *NeurIPS*, 2017. 2, 5
- [33] Michael McCloskey and Neal J Cohen. Catastrophic interference in connectionist networks: The sequential learning problem. In *Psychology of learning and motivation*, volume 24, pages 109–165. Elsevier, 1989. 2

- [34] Seyed Iman Mirzadeh, Mehrdad Farajtabar, Razvan Pascanu, and Hassan Ghasemzadeh. Understanding the role of training regimes in continual learning. In *NeurIPS*, 2020. [2](#)
- [35] Sudhanshu Mittal, Silvio Galesso, and Thomas Brox. Essentials for class incremental learning. In *CVPR*, 2021. [2](#), [3](#), [5](#), [6](#), [7](#), [8](#)
- [36] Sylvestre-Alvise Rebuffi, Alexander Kolesnikov, Georg Sperl, and Christoph H Lampert. icarl: Incremental classifier and representation learning. In *CVPR*, 2017. [2](#), [3](#), [5](#)
- [37] Anthony Robins. Catastrophic forgetting, rehearsal and pseudorehearsal. *Connection Science*, 7(2):123–146, 1995. [2](#)
- [38] Hadi Salman, Andrew Ilyas, Logan Engstrom, Ashish Kapoor, and Aleksander Madry. Do adversarially robust imagenet models transfer better? In *NeurIPS*, 2020. [2](#)
- [39] Baifeng Shi, Dinghui Zhang, Qi Dai, Zhanxing Zhu, Yadong Mu, and Jingdong Wang. Informative dropout for robust representation learning: A shape-bias perspective. In *ICML*, 2020. [3](#)
- [40] Guangyuan Shi, Jiabin Chen, Wenlong Zhang, Li-Ming Zhan, and Xiao-Ming Wu. Overcoming catastrophic forgetting in incremental few-shot learning by finding flat minima. In *NeurIPS*, 2021. [2](#)
- [41] David Stutz, Matthias Hein, and Bernt Schiele. Relating adversarially robust generalization to flat minima. In *ICCV*, 2021. [2](#), [7](#)
- [42] Xiaoyu Tao, Xinyuan Chang, Xiaopeng Hong, Xing Wei, and Yihong Gong. Topology-preserving class-incremental learning. In *ECCV*, 2020. [4](#), [5](#)
- [43] Dimitris Tsipras, Shibani Santurkar, Logan Engstrom, Alexander Turner, and Aleksander Madry. Robustness may be at odds with accuracy. In *ICLR*, 2019. [3](#)
- [44] Shikhar Tuli, Ishita Dasgupta, Erin Grant, and Thomas L Griffiths. Are convolutional neural networks or transformers more like human vision? *arXiv preprint arXiv:2105.07197*, 2021. [8](#)
- [45] Riccardo Volpi, Hongseok Namkoong, Ozan Sener, John C Duchi, Vittorio Murino, and Silvio Savarese. Generalizing to unseen domains via adversarial data augmentation. In *NeurIPS*, 2018. [2](#), [3](#)
- [46] Yue Wu, Yinpeng Chen, Lijuan Wang, Yuancheng Ye, Zicheng Liu, Yandong Guo, and Yun Fu. Large scale incremental learning. In *CVPR*, 2019. [2](#)
- [47] Mingyang Yi, Lu Hou, Jiacheng Sun, Lifeng Shang, Xin Jiang, Qun Liu, and Zhiming Ma. Improved ood generalization via adversarial training and pretraing. In *ICML*, 2021. [2](#), [3](#)
- [48] Pei Yu, Yinpeng Chen, Ying Jin, and Zicheng Liu. Improving vision transformers for incremental learning. *arXiv preprint arXiv:2112.06103*, 2021. [8](#)
- [49] Friedemann Zenke, Ben Poole, and Surya Ganguli. Continual learning through synaptic intelligence. In *ICML*, 2017. [2](#)
- [50] Hongyi Zhang, Moustapha Cisse, Yann N Dauphin, and David Lopez-Paz. mixup: Beyond empirical risk minimization. In *ICLR*, 2017. [2](#)